

## ORIGINAL ARTICLE

# The Discovery of Putative Small Molecules via Ligand-based Pharmacophore Modelling Targeting Human Tau Protein for an Effective Treatment of Parkinson's Disease

Yahaya Sani Najib<sup>1,2</sup>, Yusuf Oloruntoyin Ayipo<sup>1,3</sup>, Waleed Abdullah Ahmad Alananzeh<sup>1</sup>, Mustapha Muhammed<sup>4</sup>, Mohd Nizam Mordi<sup>1</sup>

<sup>1</sup> Centre for Drug Research, Universiti Sains Malaysia, USM 11800, Pulau Pinang, Malaysia

<sup>2</sup> Department of Pharmaceutical and Medicinal Chemistry, Bayero University Kano, PMB 3011, Kano Nigeria.

<sup>3</sup> Department of Chemistry, Kwara State University, Malete, PMB 1530, Ilorin, Nigeria

<sup>4</sup> Department of Clinical and Social administrative Pharmacy Universiti Sains Malaysia, USM 11800, Pulau Pinang, Malaysia

## ABSTRACT

**Introduction:** The human tau protein is a key protein involved in various neurodegenerative disease (NDs) including Parkinson's disease (PD). The protein has high tendency to aggregate into oligomers, subsequently generating insoluble mass in the brain. Symptoms of PD include tremor, bradykinesia, rigidity, and postural instability. Currently drugs for PD treatment are only symptom-targeted while effective therapeutic treatment remains a challenge. The objective of this study is to identify novel promising anti-PD drugs using computational techniques. **Method:** ligand-based (LB) receptor modelling was conducted using LigandScout, validated and subjected to Glide XP docking, virtual screening, ADMET, and molecular dynamics predictions. **Results:** The adopted LB modelling generated pharmacophoric features of 5 hydrogen bond donors, 1 aromatic rings, and 7 hydrogen bond acceptors. The validation result indicated GH score of 0.73 and EF of 36.30 as validation protocols, probing it to be an ideal model. Using 3D query of the modelling a total of 192 compounds were retrieved from interbioscreen database containing 70,436 natural compounds. Interestingly, ligands 1, 2, 3, 4 and 5 orderly indicated higher binding affinities to the receptor with Glide XP docking of -7.451, -7.368, -7.101, -6.878, and -6.789 compared to a clinical drug Anle138b with -4.552 kcal/mol respectively. Furthermore, molecular dynamics and pkCSM pharmacokinetics demonstrated ligands 1, 2, & 4 having better stability and low toxicity profiles compared to the reference. **Conclusion:** In summary, the study pave way for discovery of small molecules that could be recommended as adjuvant /single candidate as ant-PD candidates upon further translational study.

*Malaysian Journal of Medicine and Health Sciences* (2023) 19(6):83-94. doi:10.47836/mjmhs.19.6.12

**Keywords:** Ligand-based modelling; Human tau protein; Parkinson's disease; aggregation; virtual screening

## Corresponding Author:

Sani Yahaya Najib, PhD

Email: najibsani62@student.usm.my,

Tel: +601120988567

## INTRODUCTION

A number of neurodegenerative diseases (NDs) share proteopathic characteristics, specifically alpha-synuclein ( $\alpha$ -synuclein) protein. Misfolding and aggregation of this soluble protein leads to formation and propagation of toxic soluble debris appearing as insoluble fibrillar structure called  $\beta$ -sheet. Parkinson's disease (PD) is a NDs having symptoms including resting tremor, bradykinesia, appearing at initial stage of the disease while postural instability appears when fibrillar structures of  $\alpha$ -synuclein are formed at the terminal stage of the disease (1). Early discovery of

$\alpha$ -synuclein protein as a precursor protein for non  $\beta$ -amyloid component of Alzheimer's disease (AD) plaques, makes it an interesting protein in NDs. Recent advance techniques such as immunohistochemistry and immuno electron spectroscopy have identified  $\alpha$ -synuclein as the major component of Lewi's body and Lewi's neurites, indicating it as pathological hallmark in NDs including dementia with Lewi's body and PD (2, 3). Moreover, cyclin dependent kinase enzymes play key role in neuronal development and function. The cyclin dependent kinase 2 (cdk2) is conserved and highly expressed in the neurons, and its activity is increased upon injection of 1-methyl-4-phenyl-1,2,3,6-tetrahydropyridine (MPTP), a toxin responsible for damaging dopamine neurons and subsequent neurodegeneration causing PD (4).

Mounting evidences suggest that pathogenesis of PD is

associated with  $\alpha$ -synuclein especially, the toxic  $\beta$ -sheet that are considered soluble oligomer complexes, rather than fibrils, which are essential component of Lewy's body (5). Among various proteopathic proteins, human tau protein is considered key in the pathogenesis of PD. It has high tendency to aggregate fast and form fibrillar insoluble structures within the brain (1). Furthermore, other evidences indicates that tau protein undergoes polymerization through utilization of inducers and phosphorylation of  $\alpha$ -synuclein. Hence, due to its unique characteristics and implication in PD pathogenesis, the toxic  $\beta$ -sheet of Human tau protein is considered a therapeutic target for treatment of PD (1). Most cases of PD are sporadic and several mutations are linked to inherited forms of PD. Mutations due to leucine-rich repeat kinase 2 (LRRK2) is the most common autosomal and familial form of PD. The LRRK2 is a long AA with dominant region link to GTPase enzyme, the kinase domain is similar to serine/threonine protein kinase involves in cell cycle control. The human cyclin A3 or the human tau acts at GTPase to aid initiation of DNA synthesis in LRRK2 leading to PD (1). Thus, the human tau (4EOM) was used in this study.

Numerous natural compounds have been documented to improve cognitive functions and neurological conditions in human body. Many of such potential natural products with lesser side effects, cost-effectiveness, and environmentally friendly are still unexplored. Nevertheless, finding a therapeutic compounds targeting PD is costly and time consuming to develop a novel compound. Therefore, application of computational approach provides high resolution state and parameters that could be used to screen large set of compounds, minimizing cost, waste of resources, and eliminate candidates having poor adsorption, distribution, metabolism, excretion and toxicity (ADMET) properties (6, 7).

The aim of this research is to develop ligand-based pharmacophore model that could be use to selectively screen and pick novel anti-PD compounds from large interbioscreen (IBS) database containig naturally occuring plant compounds . The putative retrieved ligands were evaluated theroretically against toxic  $\beta$ -sheet of Human tau protein using maestro Glide extra precision (XP) docking, ADMET prediction via machine-learning graph-based pkCSM pharmacokinetics server, while stabilities against the toxic oligomers were virtually simulated using molecular dynamic simulation (MD). Finally identified hits represent promising toxic oligomers inhibitors for that could be subjected to further transtional study for effective treatment of PD.

## MATERIALS AND METHODS

### Ligand-based pharmacophore model generation

Applying the default settings function of LigandScout 4.4 software <http://www.inteligand.com/cgi-bin/>

[ligandscout4/register.pl](http://www.inteligand.com/cgi-bin/ligandscout4/register.pl), which means imporyting the SDF format of the ligands into LigandScout followed by clustering through a pharmacophoric fingerprint mapping. After that, the clustered compounds were aligned by selecting conformers with the highest cluster identification number and cluster size to develop hypothesis models (1-10), using pharmacophore radial distribution function (RDF) code similarity that is embedded in LigandScout (8). Pharmacophore models were generated, which is an essential tool for advance molecular design (9, 10). To effectively generate ligand-based pharmacophore model, known inhibitors of Human tau protein, which serves as training set (Fig. S1) were obtained from different literatures (11-16). The structural formula and the smiles of the ligands were obtained from pubchem database (<https://pubchem.ncbi.nlm.nih.gov/>) and imported into the LigandScout as mentioned above. Pharmacophore features of the models were then generated.

### Validation of Pharmacophore modelling

Validation protocol is key for an efficient and accurate model generation. The model was validated for Gunner-Henry's good hit (GH) scoring function, optimum specificity (SP), sensitivity (SE), area under the curve in Receiver Operating Characteristics (ROC), and enrichment factor (EF) for accuracy and reliability of the model. A good model should adequately discriminate between active from decoy sets by displaying high SE and error reduction between the actives and decoys. Firstly, the decoy sets were virtually generated using online decoy finder (<http://URVnutrigenomica-CTNS.github.com/DecoyFinder>) (17). Each of the model generated was used to screen the database of the active and decoy sets (validation set) and the enlisted validation parameters were evaluated using the following equations (18)

$$\begin{aligned} \text{GH} &= [\text{Ha} (3\text{A} + \text{Ht})]/4\text{HtA} + [1 - \text{Ht} - \text{Ha}/\text{D}-\text{A}] \quad (\text{i}) \\ \% \text{Y} &= \text{Ha}/\text{Ht} \times 100 \quad (\text{ii}) \\ \text{EF} &= \text{Ha}/\text{Ht} \div \text{A}/\text{D} \quad (\text{iii}) \\ \% \text{A} &= \text{Ha}/\text{A} \times 100 \quad (\text{iv}) \end{aligned}$$

Where Y is percentage yield, A total actives, D total decoys (in-actives), Ht total hits, Ha true positive respectively.

A total of 737 compounds from IBS were obtained for discrimination between actives and in actives ligands. Of the 737 total compounds, 17 are active while 720 are decoy sets or inactive compounds obtained from directorate of decoy finder (<http://URVnutrigenomica-CTNS.github.com/DecoyFinder>) (19). Using the LigandScout internal generator database, the compounds were converted to ligand database format (.ldb) from sdf format. Physicochemical properties of decoy set including molecular weight, hydrogen bond acceptors (HBA), hydrogen bond donors (HBD), and quantity of rotatable bond must be similar to that of the ligands in

the modeling process.

### Virtual screening

Virtual database screening is an important technique in selecting potential lead compounds that could effectively inhibit toxic  $\beta$ -sheet of Human tau protein (20). The validated model having cumulative validation results was subjected to virtual screening to pick potential hits from IBS database <https://www.ibscreen.com/> containing 70,436 compounds and then screened using screening perspective embedded in the LigandScout as 3-dimensional query (3D) to retrieve potential lead compounds. Only compounds that satisfy all pharmacophoric features were retained. To check scoring functions and retrieval mode indicating pharmacophore fit" of the ligands, default parameters of LigandScout was set.

### Molecular Docking study

#### *Preparation of protein and generation of Grid Box*

The toxic  $\beta$ -sheet of Human tau protein was retrieved from protein data bank <https://www.rcsb.org/structure/4EOM> (PDB ID 4EOM). The structure was prepared using preparation wizard in Maestro interface (Protein preparation, Schrodinger, LCC, New York, NY, 2019); aimed at checking peptide bond orders, charges, and missing hydrogen atoms. In addition, ionization and optimization of the protein structure was done using OPLS3e force field with implicit solvation. The protein was subjected to minimization process until an average root mean square deviation (RMSD) reaches 0.3 Å for heavy atoms. The Human tau protein has four chains A, B, C, & D. Chain A and B, C and D were arranged in anti-parallel order via hydrogen bond. Chain A, B, water molecules, heteroatoms, and inorganic phosphate were removed. Grid dimension for binding site of the ligands was identified using site Map and amino acids (AA) present in dimer of the toxic  $\beta$ -sheet of Human tau protein. The coordinates of human tau protein dimer (toxic  $\beta$ -sheet of Human tau protein) were taken as 2.4, -21.55 and -17.59 Å representing X, Y and Z axis (21, 22).

#### *Ligands Preparation*

Using Lig PreP panel on Maestro (LigPreP, Schrodinger, LCC, New York, NY, 2019), all the hit compounds (79) from virtual screening, positive compound (Dopamine), and a known pre-clinical drug (Anle 138b), were visualized and checked for bond orders. Finally missing hydrogen atoms added, optimized the structures, and their energies minimized using OPLS3e force field and other protocols as adopted from some previous works. (18, 23) The ligands prepared were saved in SDF file output

#### *Molecular Docking study*

The final minimized protein (toxic  $\beta$ -sheet of Human tau protein) from protein preparation wizard and the

prepared ligands including the positive drug (Dopamine and Anle138b) were subjected to molecular docking study using Maestro 12.2 (Ligand docking, Schrodinger, LCC, New York, NY, 2019). The protein was refined for bond orders, missing hydrogen, formal charges, and terminal amide was added. Subsequently, protein structure with ionization state was generated. Using ligand docking panel on the Maestro, the ligands were then loaded and subsequently, docked against the prepared protein using extra precision (XP). The docking results of the ligands and the reference were ranked based on displayed energies of docking scores and selectivity against toxic  $\beta$ -sheet of Human tau protein. Poses with the most negative binding energies (favourable binding) were identified and selected for further analyses such as *in silico* ADMET predictions and MD simulation.

### In-silico Blood-Brain-Barrier Permeation and ADMET properties and Toxicity studies

#### *In-silico Blood-Brain-Barrier Permeation and ADMET properties*

In PD, drugs need to cross the Blood-Brain-Barrier (BBB) before eliciting its pharmacological response. Developing new drug molecules is challenging, costly, and risky due to low success rate of ADMET properties for potential hits compound (24). A canonical smile of each selected ligand and reference molecules were inputted into the server and the ADMET prediction mode was selected. ADMET parameters including lipophilicity (LogP), molecular weight (MW), solubility (LogS), HBA, HBD, topological polar surface area (TPSA), and flexibility of the selected ligands were extrapolated to ensure adequate transportation to the target site and pharmacological effects. Permeation via BBB and ADMET properties were computed using machine-learning graph-based pharmacokinetics server (pk-CSM pharmacokinetics server), where numerous parameters essential for accessing BBB permeation, toxicity and pharmacological effects of the ligands were determined. Such important parameters include distribution, BBB permeability, lipophilicity, *in vivo* absorption, total clearance, and toxicity (25).

#### *Toxicity studies*

The lethal Dose 50 % (LD50), which corresponds to half quantity of a compound required to kill half number of the total animals utilised in the experiment and toxicity class of each compound was determined using Pro Tox-II server. Toxicity classes are divided into six categories viz: (1) death of an Animal occurs upon swallowing 5 mg or below ( $LD50 \leq 5$  mg), (2) indicates fatality within 5-50 mg, ( $5 < LD50 \leq 50$ ), (3) denotes toxic state when injecting 50-300 mg ( $50 < LD50 \leq 300$ ), (4) the fourth class determines harmful effects of a compound at 300-2000 mg dose of the drug ( $< 300 LD50 \leq 2000$ ), (5) this class indicates weather a given compound is harmful in the dose range of 2000-5000 mg ( $< 2000 LD50 \leq 5000$ ), and the (6) class of toxicity demonstrates safety

of a compound in more than 5000 mg dose of the drug (LD50 < 5000) (26, 27). The toxicity of the compounds was analyzed and considered before selecting final compounds for further analysis.

### Molecular Dynamics

Molecular dynamics (MD) simulation was performed for the top selected five ranking compounds using academic version of Desmond 2020-3, Maestro-Desmond interoperability Tools, Schrodinger, New York, NY, 2021 (28, 29) to further confirm the binding affinity and stability of the ligand-complexes. Firstly, for placing the ligand-complexes into the orthorhombic box, system builder was used having 10 D buffer regions between box sides, protein atoms, and then filled with an appropriate single point charged water molecules. This was followed by neutralising the system with sufficient quantity of (Na + Cl-) as counter ions and fixed salt concentration of 0.15M, mimicking the physiological monovalent ion concentrations (30). To minimize any unfavourable interactions that might occur during the model builder energy minimization was applied using OPL3e force field on the fully solvated and neutralised system. The pressure and temperature were kept at constant to 1.01325 bar and 300K respectively, for isobaric-isothermal ensemble (31, 32). To regulate temperature and pressure nose-Hoover thermostat and Martyna-Tobias-Klein algorithm was employed. Similarly, a cut-off radius of 9 D was employed for short-range Van der waals and coulomb interactions, while particle mesh Ewald method was used for the accurate and efficient evaluation of electrostatic interactions.

A total of 50 nanoseconds were performed with 1000 frames for recording the trajectories. At the end of the simulation diagram tool of Desmond package was used to analyse the trajectory files (30). Some of the output recorded include root mean square deviation (RMSD), root mean square fluctuation (RMSF), radius of gyration (Rg), and statistics of hydrogen bond interactions (29, 33).

## RESULTS

### Generation of 3D pharmacophore model

Steric and electronic features of ligands are represented as a pharmacophore modelling. In this research, the models generated were based on pharmacophoric features (steric and electronic) present in the training set consisting of 10 compounds. Ten (10) hypotheses of the pharmacophore modelling were built having 1.0 tolerance scale and ranked following pharmacophore-Fit score (33). The features of a model are not only necessary to inhibit targeted protein but should have ability to bind to the binding pocket. Thus, 10 hypotheses were carefully evaluated and one of the hypotheses (Model-2) having 13 features (Fig. 1A) demonstrated best pharmacophoric features with reasonable specificity and selectivity.

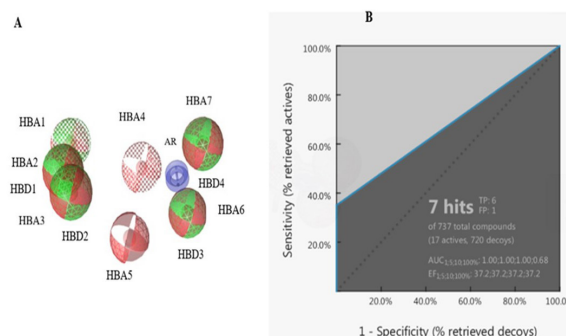


**Figure 1: Model generated and its validation: (A) Chemical features of ligand-based pharmacophore model consisting of 5 hydrogen bond donors (pink), 1 aromatic rings (blue), and 7 hydrogen bond acceptors (light green). (B) ROC curve of the validated pharmacophore model.**

### Validation of pharmacophore modelling

The LigandScout generated ten (10) models, using set of 17 known active inhibitors of  $\alpha$ -synuclein and their decoys set consisting of 720 inactive compounds, model-2 was able to retrieve 6 actives (35 %) and 1 decoy (< 1 %), while other nine models failed validation test. The model-2 was validated using two set of parameters. Firstly, GH scoring method for evaluation of reliability and accuracy of the modelling. Generally, GH ranges from 0 to 1 indicating null to an ideal modelling hypothesis respectively. Higher score of GH indicates acceptability of the pharmacophore model generated, moreover, a model with GH score from 0.6 and above is considered reliable for screening large set of databases (23, 34). In this research GH of 0.73, corresponds to the acceptable limit of validation. The second validation method, involves the application of EF to evaluate sensitivity (SE) and specificity (SP) of the model. In this research an EF value of 36.30 was obtained as validation protocol. Generally, EF value from 20 are considered good for validation protocols (34, 35). It is important for the decoy sets to discriminate between active and decoy sets for SP. The receiver operating characteristics (ROC) curve (Fig. 1B), indicated SE of the retrieved compounds and discrimination of actives from decoy sets. The result of validation is presented in Table I. Both EF and GH were computed using the following formula

$$GH = [(TP/4HtA) (3A + Ht) \{1 - (Ht - TP) / (D - A)\}] \quad (1)$$

$$EF = [(TP \times D) / (Ht \times A)] \quad (2)$$

In summary, the hypothesis yielded EF value of 36.30 and GH score of 0.73, validating the model as good. Using the generated features of the validated model, hit compounds were retrieved from IBS database.

### Pharmacophore-based virtual screening

Virtual screening of pharmacophore models is an important technique for obtaining potential lead compounds that could be developed as potential alternative drugs for disease treatment including PD.

**Table I: Validation parameters of the shared feature pharmacophore model**

S/No	Parameters	value
1	Total molecules in database (D)	720
2	Total number of actives in database (A)	17
3	Total Hits (Ht)	7
4	True Positive (TP)	6
5	% Yield of actives {(TP/Ht)100}	35.29
6	True negatives (TN)	0
7	False-negative (FN) = [A-TP]	11
8	False-positive (FP) = [Ht-TP]	1
9	Sensitivity (SE) = TP/A	0.35
10	Specificity (SP) = TN/D-A	0
11	Enrichment factor (EF) = {(TPxD)/(HtxA)}	36.30
12	Accuracy = (TP + TN)/(TP + TN + FP + FN)	1
13	Goodness of hit score (GH) = [(TP/4HtA) (3A + Ht) (1_(Ht-TP)/(D-A))]	0.73

The ability of the hypotheses to discriminate between active and inactive ligands highlights knowledge of the molecules required for new candidate compounds (20). Model-2 was validated having mapping it with validation set consisting of active ligands and decoys. Subsequently, the 3D query of the model identified 192 hits from IBS database containing 70,436 natural product compounds. The 192 ligands were then subjected to molecular docking analysis.

### Molecular docking

Reduction of false positive and identification of suitable orientation of ligands at the binding pocket is essential in identifying new drug-like molecules, thus application of molecular docking study (36). The prepared toxic

huma tau  $\beta$ -sheet protein was uploaded as target during molecular docking and the docking analysis was performed on the protonated conformers. Binding site of the ligands was defined within 1.0 E radius and RMSD was set at 0.3 E. The docking protocol was validated through re-docking of the co-crystallized ATP ligand within the binding pocket of the protein. The re-docked ATP produced a root mean square deviation (RMSD) of 0.216 E. The binding interaction demonstrated by the redocked ATP is similar to its reported interactions in RCSB PDB (Fig. 2 A) and similar interactions with the selected ligands were observed especially, at hydrogen bond interactions with AA residues Gln C3, Lys D7, and Glu C9 (Table II). Secondly, having an RMSD

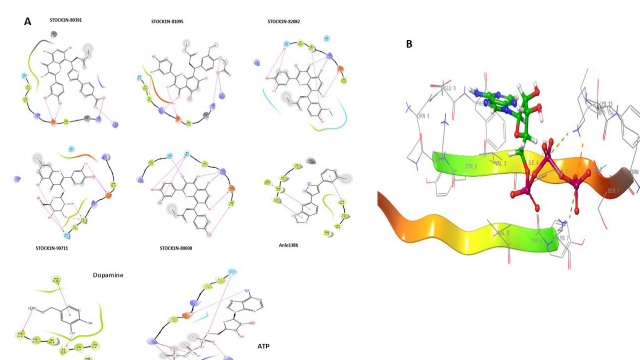


**Figure 2: Interactions of the ligands and various amino acid residues. (A) Binding poses of the selected ligands and reference Anle138b indicating bonding and non-bonding interactions of the selected ligands with amino acid residues in the active pocket of the receptor. Hydrogen bonding (magenta arrow),  $\pi$ -cation (red line), and  $\pi$ - $\pi$  stacking (green line) (B) Re-docked ATP showing interactions with various AA residues**

**Table II: Binding affinity of selected ligands and reference compound**

Ligands	Docking score (kcal/mol)	Glide gscore (kcal/mol)	Glide energy (kcal/mol)	XP Gscore (kcal/mol)	Interactions	
					H-bond	Others
STOCK1N-80391 (1)	-7.451	-7.461	-44.466	-7.461	Glu C9, Lys D7	Lys C13 (salt bridge)
STOCK1N-81095 (2)	-7.368	-7.381	-36.238	-7.381	Val C5, Lys C7, Glu C9, Lys C13	Lys D7 (salt bridge)
STOCK1N-82082 (3)	-7.101	-7.161	-39.172	-7.161	Gln D3, Val D5, Lys D7, Glu D9	Lys D7 (salt bridge)
STOCK1N-99711 (4)	-6.878	-6.907	-40.453	-6.907	Gln D3, Val D5, Glu D9	---
STOCK1N-80698 (5)	-6.789	-6.849	-31.386	-6.849	Gln C3, Gln D3, Lys D7, Glu D9, Phe D10	Lys D7 (salt bridge)
STOCK1N-80317 (6)	-6.471	-6.532	-37.847	-6.532	Gln D3, Val D5, Glu D9, Gln C3,	Lys D7, Lys C7 (salt bridge)
STOCK1N-81413 (7)	-6.065	-6.97	-38.148	-6.97	Gln D3, Val D5, Gln C3, Lys D7, Glu D9	Lys D7 (salt bridge)
STOCK1N-83099 (8)	-5.589	-5.605	-42.471	-5.605	Val5, Lys7, Glu9,	---
STOCK1N-83408 (9)	-5.559	-5.572	-43.8	-5.572	Gln D3, Val D5, Lys D7, Glu D9, Gln C3	---
STOCK1N-44373 (10)	-5.544	-5.664	-19.843	-5.664	Ile C4	Phe C10 ( $\pi$ - $\pi$ stacking)
Anle138b	-4.552	-4.963	-22.953	-4.963	---	Tyr C6, Tyr D6, Phe D10
Dopamine	-4.992	-4.992	-14.209	-4.992	Ile C4	Phe D10, Tyr D6
ATP	-5.436	-5.508	-60.186	-5.508	Gln C3, Lys D7, Glu C9	Lys C13

Note: **Docking scores** indicates function of binding affinity specific to a ligand, program and energy function, high negative value indicates strong binding. **Glide Gscore** demonstrate empirical scoring function indicating binding affinity of the ligands, **XP Gscore** indicates extra precision of binding affinities of the ligands to receptor and takes more time, **Glide energy** show ligand binding free energy and it indicates force field energies such as electrostatic and Van der waals, influencing ligand binding

value within the acceptable range of  $\leq 2.0$  validates the docking protocols as reliable. The docked ATP with the protein is presented in Fig. 2 B. The prepared hits (192) and the reference compounds were selected based on their binding energies, higher negative value indicate better binding affinity, ligands displaying high binding affinity were compared to the reference compound and selected for further analysis. The reference compound Anle138b demonstrated none hydrogen bonding but indicated good pi-pi ( $\pi-\pi$ ) stacking with TYR C6, TYR D6 and PHE C10. Interestingly, the first five compounds (Table II) demonstrated higher energy and binding potentials than the reference compound. The discovered small molecule compounds namely; STOCK1N-80391 (1), STOCK1N-81095 (2), STOCK1N-82082 (3), STOCK1N-99711 (4) and STOCK1N-80698 (5) orderly showed higher binding energy affinity and potentials for stronger activity against the toxic  $\beta$ -sheet Human tau protein compared to the reference (Anle138) and positive compound (dopamine). Furthermore, the ligands were shown to have strong hydrogen bond interactions at chain D with key AA residues such as Val C5, Glu D9, Lys D7, Glu D9, and Phe D9 respectively through C=O and O bonds. The binding poses of the ligands (Fig. 2 A) demonstrated a better binding and interactions of the ligands with specific bond site of the protein. The selected top best five compounds demonstrated similar binding pocket and AA interactions from the docking conformation of the hit as demonstrated in Fig. 2 A. The selected small molecules demonstrated a good strength as a result of positive fitting into the active cavity of

the protein. Compounds 3, 4, and 5 had shown similar hydrogen interactions with Gln D3 and Glu D9 AA residues through OH bonds with similar salt bridge except ligand 4. Similarly, ligands 1 & 2 established similar interactions at C-terminal of the protein interacting with AA Glu C9 and Lys D7 through OH bonding, Lys D7. Ligands 1 & 2 demonstrated strong affinity through C=O and O bond respectively. Generally, the compounds demonstrated higher and broader binding affinity comparable to Dopamine and Anle138b reference compounds with an interesting interaction making them potential drug-like candidates. Therefore, the selected ligands and the positive references were subjected to ADMET and molecular dynamics trajectories for further analysis and interaction with the receptor.

### In-silico Blood-Brain-Barrier permeation and ADMET screening

The selected ligands retrieved from molecular docking were subjected to ADMET properties. The ADMET is crucial parameters for pharmacological response and are employed to successfully identify potential lead compounds with sufficient properties such as drug-like properties, molecular weight, BBB, and central nervous system (CNS) permeability (37). One of such robust and validated online servers for pharmacokinetics is a machine-learning graph-based pharmacokinetics server known as pk-CSM pharmacokinetics pkCSM (uq.edu.au). In this study, a number of ADMET properties including chemical properties of the ligands (Table III A) were predicted to screen the drug-likeness properties of

**Table III A & B: Physicochemical properties of the selected ligands (A) Chemical properties of the selected compounds (B) pharmacokinetic and pharmacodynamic properties of selected compounds on Human tau protein**

Descriptor	Compounds and values						
	1	2	3	4	5	Dopamine	Anle138b
Molecular weight <sup>a</sup>	573.486	567.479	508.435	464.379	478.409	153.18	343.18
LogP <sup>b</sup>	3.3065	1.8203	2.1332	-0.5389	2.1246	0.599	4.2349
#Rotatable bonds <sup>c</sup>	7	9	6	4	5	2	2
#Acceptors <sup>d</sup>	12	13	11	12	10	3	3
#Donors <sup>e</sup>	5	5	4	8	4	3	1
Surface area <sup>f</sup>	235.072	230.177	208.172	183.901	196.694	65.090	129.397
Lipinski's Rule of 5	0	0	0	0	0	0	0

<sup>a</sup>Molecular weight (acceptable range < 500)

<sup>b</sup>Lipophilicity acceptable range 1.35-1.80)

<sup>c</sup>Number of rotatable bonds (acceptable range  $\leq 10$ )

<sup>d</sup>Hydrogen bond acceptors (acceptable range  $\leq 10$ )

<sup>e</sup>Hydrogen bond donors (acceptable range < 5)

<sup>f</sup>Octanol/water partition coefficient (acceptable range < 70 E)

### B

COMPOUND	QPlogS <sup>a</sup>	Caco2	IA <sup>b</sup>	Log VDss <sup>c</sup>	QPlogKp <sup>d</sup>	LogBB <sup>e</sup>	LogPS <sup>f</sup>
STOCK1N-80391(1)	-2.898	-0.628	61.112	-0.549	-2.735	-2.05	-4.322
STOCK1N-81095 (2)	-2.897	-0.517	61.221	0.101	-2.735	-2.217	-4.18
STOCK1N-82082 (3)	-3.276	0.423	90.867	-0.298	-2.735	-1.512	-3.716
STOCK1N-99711 (4)	-2.949	-0.878	38.815	0.414	-2.735	-2.098	-4.65
STOCK1N-80698 (5)	-3.475	0.033	85.573	-0.566	-2.735	-1.381	-3.584
<b>Anle138b</b>	-3.363	1.308	92.057	0.226	-2.736	0.353	-1.157
<b>Dopamine</b>	-0.887	0.716	75.815	0.622	-2.863	-0.414	-2.65

<sup>a</sup>Predicted aqueous solubility S in mol l<sup>-1</sup> (acceptable range -6.5 to 0.5)

<sup>b</sup>Predicted Human intestinal absorption (acceptable range > 30 %)

<sup>c</sup>Predicted steady state volume of drug distribution (acceptable range -0.15 to 0.45)

<sup>d</sup>Predicted skin permeability (acceptable range < -2.5)

<sup>e</sup>Predicted blood-brain barrier permeability (acceptable range -1.0 to 0.3)

<sup>f</sup>Predicted central nervous system permeability (acceptable range -3.0 to -2.0)

the ligands as potential hits including aqueous solubility (Log S), total surface polar area (TSPA) octanol/water partition coefficient (QPlog Po/w), skin permeability (QP Log Kp) and Lipinski's rule of five (25). The Lipinski's rule of 5 is reliable evidence for predicting compounds as an ideal orally available drug (38). The ligands have number of rotatable bonds  $\geq 145$  E, indicating optimal flexibility. Interestingly, all the selected compounds have passed the rule; therefore, concentrations of the ligands could be adequately maintained within human system. The selected compounds display competitive physicochemical properties including lipophilicity, flexibility, saturation, polarity, and solubility as drug-like compounds. The discovered small molecules shortlisted namely are; STOCK1N-80391 (1), STOCK1N-81095 (2), STOCK1N-82082 (3), STOCK1N-99711 (4) and STOCK1N-80698 (5) having desirable and acceptable range of physicochemical properties that could be regarded as potential drug-like compounds. The ligands exhibited physicochemical parameters within an acceptable range, for instance MW 480-580, number of rotatable bond 5-9, HBA 10-13, and HBD 4-8. However, few deviations of these properties were observed, compound 2 indicated the highest desirable lipophilic properties comparable to reference compound. Most of the hit compounds have desirable properties that could be considered and developed as potential anti-PD drugs as druggable compounds (39).

Permeability to cross the BBB is a complex process that involves transcellular passive and active diffusion processes. Thus, drugs that could be developed as anti-PD agents must cross the BBB actively or passively (40). Compounds with MW > 500 Da and TSPA < 70 E are said to cross the BBB through passive diffusion, while others cross via active transport system (24, 41). The selected compounds indicated ability to pass the BBB actively. Therefore, compounds having such properties could be considered for further translational evaluation as potential anti-PD agents. Parameters such as pharmacokinetics and pharmacodynamics of the selected compounds (Table III B) provide sufficient evidences for considering these ligands as potential druggable compounds. Moreover, providing an insight on how to avoid unwanted side effects during evaluation of the compounds as potential anti-PD compounds.

Additionally, parameters that are essential in evaluating bioavailability of compounds are human intestinal absorption and Caco-2 permeability. The selected ligands displayed a sufficient value that could be considered essential in evaluating bioavailability. The compounds have indicated sufficient percentage of absorption via human intestine when administered orally except ligand 4 with minor deviation. Compound 3 and Anle138b demonstrated greater than 90 % predicted absorption. Generally, ligands displayed good aqueous solubility and low Caco-2 permeability, indicating ease of absorption through human intestine (42). Similarly,

steady volume of distribution was observed, indicating uniform concentration of compounds in plasma when administered, except ligand 1 & 5 with minor deviation. This reveals the importance of theoretical dose needed to distribute any drug in plasma and tissue in accessing druggable compounds. For screening NDs drugs, another important ADMET parameter is the ability of the compounds to cross BBB and CNS, ligands 5, 3, 1, 4 and 2 demonstrated favorable conditions to cross the BBB in an ascending order respectively, comparable to the reference compounds (Anle138b and dopamine) having less compared to the ligands. Infact, 5 & 3 ligands displayed better CNS permeability and lipophilic tendencies as compared to reference Anle138b and positive drug dopamine. Therefore, the selected compounds could have potential to transit across the BBB in order to elicit their pharmacological effect. Although, presence of tertiary nitrogen is desired predictor in a compound for CNS penetration and a higher degree of permeability to BBB, the selected compounds demonstrated no any nitrogen atom as a major interactions with relevant AA and this could be considered as a strong structural activity relationship point that could be explored for better penetration to the brain (43). It was observed from the pharmacokinetics parameters, the selected ligands especially 1, 2, 3, & 4 could have little or no interference with drug metabolism, distribution, and toxicity due to inability to affect Cytochrome P450 enzyme, thus, indicating potentiality of these compounds as druggable like candidates. Ligands 5, 3 & 4 were predicted to have better total drug clearance comparable to others, indicating none renal toxicity. Although, compounds displayed good physicochemical properties, however, they are likely to cause skin sensitization as they can penetrate through skin and this could interfere against P-glycoprotein substrate enzyme (44).

All the selected ligands have no effect on hERG1, while compounds 3, 4, & 5 and reference Anle138b, might have effects on hERG2, and this could be a variable for possible delay in ventricular repolarization during cardiac rhythm (45). It is important to note that, filters such as, oral acute toxicity (LD50), hepatotoxicity and oral rat chronic toxicity (LOAEL) indicate side effects of any drug when administered in a small dose for long period of time. Interestingly, none of the ligands displayed such effects, except 4 with little deviation and this could be further evaluated. The selected compounds were carefully examined to avoid any unwanted effect during the cause of clinical evaluation as a result of inadequate ADMET deficiencies of the hits.

#### Toxicity of the selected compounds

To evaluate safety of the compounds, endpoint toxicities was studied. Ligands 1, 2, 3, & 5 belong to class 4, indicating the compounds could be harmful when swallowed in adose range of 300-2000 mg/kg (300 < LD50  $\leq$  2000). Only ligand 4 belongs to class

toxicity of 5 indicating its potential harmful effects when swallowed between 2000-5000 mg/kg dose. This data shows that ligands 1, 2, 3, & 5 could be toxic in smaller doses of 300 mg/kg. It is important to note that, filters such as LD50, hepatotoxicity and oral rat chronic toxicity (LOAEL) indicate side effects of any drug when administered in a small dose over a long period of time. Interestingly, ligands displayed similar toxicity range in both table S1 & SII and falls mostly within toxicity class 4 except compound 4 that falls within class 5 toxicity. Therefore, the ligands could be considered for further evaluation as potential anti-PD agents.

**Molecular dynamics simulations**

Molecular dynamics (MD) simulation is an indispensable tool in biophysics as it provides structural and dynamic stability of selected ligand-receptor complex. Even though, MD analysis of  $\leq 10$  ns is considered sufficient for preliminary *in silico* studies of ligand complex. In this study MD of 50 ns was run in order to propose stable compound that could be further developed as drug candidate's inhibitor against toxic  $\beta$ -sheet of human tau protein (46). The high binding affinity of compounds 1,2,3,4 & 5 observed compared to the reference showed number of H-bond (Fig. 3 A) for the compounds and this might account for higher binding energies of the compounds. This inclined contribution of hydrophilic, hydrophobic, and non-bonding interactions especially, OH and C=O bonding to polar and non-polar amino acid residues as observed in Fig. 2 A. In most cases these binding interactions contribute to drug-like properties of the potential candidates (49).

As observed in the RMSD plot (Fig 3 B), the receptor backbone was initially deviated at around 0.5-1.3 Å before becoming equilibrated at 20 ns. Subsequently, an insignificant deviation was observed up to the end of the simulation time of 50 ns. This indicates that 50 ns selected is adequate for simulation study of these compounds. At the same time the ligands enter equilibrium time condition and maintained stability throughout the simulation time. Fluctuation of RMSD between 1-3 Å throughout simulation time is considered as stable system. (28, 29).

The Apo protein analysis revealed RMSD plot ranging between 1.0 to 1.4 Å, indicating good stability of the protein. Good stability condition was observed for 1, 2, and 4, consistent or in some cases comparable to the reference (Anle138b). It was observed that for ligands to enter binding cavity of receptor, it must be supported by dynamic thermal motions, transient channels and mean square isotropic displacement, and this is represented by temperature or B-factor (Fig. 4A) and RMSF (Fig 4B). All the ligands and the reference showed insignificant fluctuation with receptor. Moreover, compound 4 and 1 showed comparable stability to the reference (Anle138b) respectively, while 2, 3, and 5 ligands fluctuate in an ascending order compared to the reference.

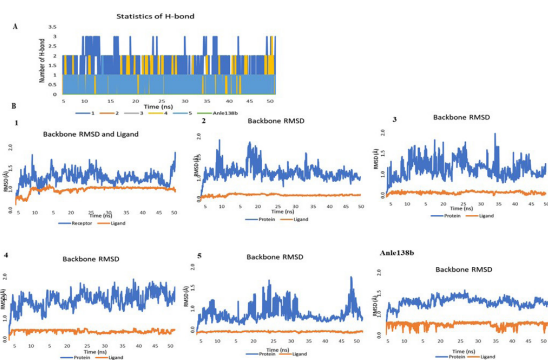


**Figure 3: Trajectories of molecular dynamic simulation: (A) Statistics of H-bond contacts between ligands and relevant amino acids at the receptor active pocket. (B) ligand and receptor backbone RMSD.**

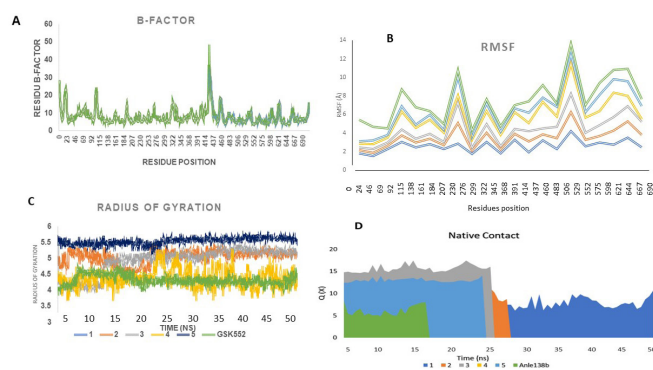


**Figure 4: Molecular Dynamics simulation results of selected ligands against Human Tau protein. (A) B-factor or temperature factor, where the lowest fluctuations are observed in 1, 2, and 3 compared to reference Anle138b. (B) is the RMSF which demonstrated similar fluctuations indicating stability of the selected ligands. (C) The radius of gyration indicating more compactness and stability of the receptor-ligand system. (D) the native contact of the receptor-ligand complex, relatively favouring the ligands due to less variations in (Q) values otherwise promoting receptor rigidity.**

Furthermore, stability and compartments of the ligand-receptor complexes were demonstrated by radius of gyration (Rg) plot (Fig. 4C), which was determined by folding state of ligand-protein complexes. Both stability and compartments of ligands and reference Anle138b were supported by Rg plot. The native contact (Q) presented in Fig. 4D, indicates stability of the complexes and it is demonstrated between the ligands, references, and receptor with folding free energies demonstrating stability of the ligands, and no unfolding by large or higher Q fluctuations was observed. Interestingly, all the ligands fluctuate at AA residues between 1-21, indicating similar pattern of fluctuations. Among the compounds, ligand 5 fluctuates more and this was illustrated in Fig. S4, which shows similar results with Fig. 4 B. The ligands of interest showed a good stability; moreover, looking at Q results ligands 1, 2, and 4 displayed least fluctuation of folding protein as observed in Q (X). Overall compound 1, 2, and 4 demonstrated better contact to folding protein, good stability and least Q fluctuation compared



to the reference Anle138b. The selected ligands demonstrated a stable ligand-receptor complexes in a folding state along the simulation trajectories. Thus, demonstrating ligands binding flexibility to receptor with better conformational state. (48, 49) Generally, the selected IBS natural product compounds (1, 2, 3, and 5) demonstrated ideal flexibility and stability to human tau protein-ligand complexes better than the reference compound Anle138b, and this further probe their potential as drug-likeness candidates.

## DISCUSSION

NDs are chronic diseases affecting mostly aged people. One of the most common NDs having multiple pathological ways is PD. Toxic  $\beta$ -sheet of Human tau protein is one of the many pathological ways causing PD. The disease has many symptoms including motor and non-motor symptoms. Among the prominent motor symptoms include tremor, bradykinesia, and postural instability. Current drugs used clinically for treating PD are symptoms-targeted and yet no curative drug available presently. Many natural products are reported to have neuroprotective effects with promising potential to treat NDs (6). The study developed and validated LB pharmacophore model which retrieved substantial number of compounds from the IBS natural product database. Importantly, the ligand-receptor complexes were developed based on LB pharmacophore model. Further evaluation of the selected small molecules using molecular docking study leads to retrieval of ligands demonstrating strong binding activity against toxic  $\beta$ -sheet of Human tau protein. The compounds indicated competitiveness to the receptor compared to the reference compound (Anle138b) and positive drug (dopamine). Examining the various pharmacological pathways and cumulative advantages of comprehensive report analysis of the selected ligands; five compounds namely 1, 2, 3, 4, and 5 were found to demonstrate better flexibility, stability, and potential to bind to toxic  $\beta$ -sheet of Human tau protein compared to the reference compound. The compounds demonstrated high affinities, stabilities and drug-likeness properties to the Human tau protein as shown by the computational analysis. Furthermore, the observed reductions in dynamic motion fluctuation of the compounds contributed to their stability, and improved binding potentials against the receptor target.

Selectively, compound 3, 4, and 5 were found to have good physicochemical properties and impressively showed good pharmacokinetics properties, druggability, low toxicity profile, and strong binding activity to that could lead to promising inhibition of the target protein compared to the reference compound (Anle138b). In summary, the study demonstrated strong binding energies, and stability that are comparable to similar compounds reported in the literature which are validated experimentally. This makes the ligand-based modelling entailed in this study reliable and build a confidence to

further undergo rigorous experiment to develop potential anti-PD drugs via activity against Human tau protein with prospects from natural compounds available in IBS database. Therefore, the selected ligands are recommended as potential and promising anti-PD small molecules that could target toxic  $\beta$ -sheet of Human tau protein for translational study, upon further biochemical analyses

## CONCLUSION

The study demonstrated application of computational approach for Ligand-based pharmacophore modelling to develop potential and strong compounds having activity against toxic  $\beta$ -sheet of Human tau protein that could treat PD. The LB modelling was successfully validated using GH Score and EF, and substantial number of hit compounds were retrieved from large IBS database containing natural compounds. Moreover, exploring the binding affinities, pharmacokinetic parameters, and MD simulation analysis including RMSD and RMSF, compounds demonstrated an ideal stability and affinities. In summary, the selected small molecule compounds via simulation analysis revealed powerful binding affinities, stabilities, and potential to bind to toxic  $\beta$ -sheet of Human tau protein. Therefore, this could serve as a model to explore therapeutically novel compounds as promising or viable candidates to treat PD and other NDs upon further experimental translation study.

## ACKNOWLEDGEMENTS

Funding by TETFUND, Nigeria for PhD program and support of grand Fundamental Research Grand Scheme (203.CDADAH.6711955), Ministry of Higher Education of Malaysia

## REFERENCES

1. Ryan P, Xu M, Jahan K, Davey AK, Bharatam PV, Anoopkumar-Dukie S, et al. Novel Furan-2-yl-1H-pyrazoles Possess Inhibitory Activity against  $\alpha$ -Synuclein Aggregation. *ACS Chem Neurosci*. 2020;11(15):2303-15. doi: 10.1021/acschemneuro.0c00252.
2. Behl T, Kumar S, Althafar ZM, Sehgal A, Singh S, Sharma N, et al. Exploring the Role of Ubiquitin-Proteasome System in Parkinson's Disease. *Molecular neurobiology*. 2022;59(7):4257-73. doi: 10.1007/s12035-022-02851-1.
3. Naoi M, Maruyama W, Shamoto-Nagai M. Rasagiline and selegiline modulate mitochondrial homeostasis, intervene apoptosis system and mitigate  $\alpha$ -synuclein cytotoxicity in disease-modifying therapy for Parkinson's disease. *Journal of neural transmission (Vienna, Austria : 1996)*. 2020;127(2):131-47. doi: 10.1007/s00702-020-02150-w.

4. Deng S, Pan B, Gottlieb L, Petersson EJ, Marmorstein R. Molecular basis for N-terminal alpha-synuclein acetylation by human NatB. *eLife*. 2020;9. doi: 10.7554/eLife.57491.
5. Xu CK, Castellana-Cruz M, Chen SW, Du Z, Meisl G, Levin A, et al. The Pathological G51D Mutation in Alpha-Synuclein Oligomers Confers Distinct Structural Attributes and Cellular Toxicity. *Molecules*. 2022;27(4). doi: 10.3390/molecules27041293.
6. Dos Santos Nascimento IJ, de Aquino TM, da Silva Júnior EF. Computer-Aided Drug Design of Anti-inflammatory Agents Targeting Microsomal Prostaglandin E(2) Synthase-1 (mPGES-1). *Current medicinal chemistry*. 2022;29(33):5397-419. doi: 10.2174/0929867329666220317122948.
7. Gurung AB, Ali MA, Lee J, Farah MA, Al-Anazi KM. An Updated Review of Computer-Aided Drug Design and Its Application to COVID-19. *Biomed Res Int*. 2021;2021:8853056. doi: 10.1155/2021/8853056.
8. Wolber G, Langer T. LigandScout: 3-D pharmacophores derived from protein-bound ligands and their use as virtual screening filters. *Journal of chemical information and modeling*. 2005;45(1):160-9. doi: 10.1021/ci049885e.
9. Marcou G, Varnek A. Relational Chemical Databases: Creation, Management, and Usage. *Tutorials in Chemoinformatics*. 2017:37-66. doi: 10.1002/9781119161110.ch2
10. Wolber G, Langer T. LigandScout: 3-D pharmacophores derived from protein-bound ligands and their use as virtual screening filters. *J Chem Inf Model*. 2005;45(1):160-9. doi: 10.1021/ci049885e
11. Ghasemi Tigan M, Ghahghaei A, Lagzian M. In-vitro and in-silico investigation of protective mechanisms of crocin against E46K  $\alpha$ -synuclein amyloid formation. *Mol Biol Rep*. 2019;46(4):4279-92. doi: 10.1007/s11033-019-04882-9.
12. Liu H, Chen L, Zhou F, Zhang YX, Xu J, Xu M, et al. Anti-oligomerization sheet molecules: Design, synthesis and evaluation of inhibitory activities against  $\alpha$ -synuclein aggregation. *Bioorg Med Chem*. 2019;27(14):3089-96. doi: 10.1016/j.bmc.2019.05.032.
13. Lu JH, Ardah MT, Durairajan SS, Liu LF, Xie LX, Fong WF, et al. Baicalein inhibits formation of  $\alpha$ -synuclein oligomers within living cells and prevents A $\beta$  peptide fibrillation and oligomerisation. *Chembiochem*. 2011;12(4):615-24. doi: 10.1002/cbic.201000604.
14. Masuda M, Suzuki N, Taniguchi S, Oikawa T, Nonaka T, Iwatsubo T, et al. Small molecule inhibitors of alpha-synuclein filament assembly. *Biochemistry*. 2006;45(19):6085-94. doi: 10.1021/bi0600749.
15. Parambi DGT, Saleem U, Shah MA, Anwar F, Ahmad B, Manzar A, et al. Exploring the Therapeutic Potentials of Highly Selective Oxygenated Chalcone Based MAO-B Inhibitors in a Haloperidol-Induced Murine Model of Parkinson's Disease. *Neurochemical research*. 2020;45(11):2786-99. doi: 10.1007/s11064-020-03130-y.
16. Zhao Y, Ye F, Xu J, Liao Q, Chen L, Zhang W, et al. Design, synthesis and evaluation of novel bivalent  $\beta$ -carboline derivatives as multifunctional agents for the treatment of Alzheimer's disease. *Bioorg Med Chem*. 2018;26(13):3812-24. doi: 10.1016/j.bmc.2018.06.018.
17. Cereto-Massagué A, Guasch L, Valls C, Mulero M, Pujadas G, Garcia-Vallvé S. DecoyFinder: an easy-to-use python GUI application for building target-specific decoy sets. *Bioinformatics*. 2012;28(12):1661-2. doi: 10.1093/bioinformatics/bts249.
18. Ayipo YO, Alananzeh WA, Yahayaa SN, Mordi MN. Molecular Modelling and Virtual Screening to Identify New Piperazine Derivatives as Potent Human 5-HT1A Antagonists and Reuptake Inhibitors. *Comb Chem High Throughput Screen*. 2022. doi: 10.2174/1386207325666220524094913.
19. Adrià CM, Garcia-Vallvé S, Pujadas G. DecoyFinder, a tool for finding decoy molecules. *Journal of cheminformatics*. 2012;4(1):1-. doi: 10.1186/1758-2946-4-S1-P2
20. Niu MM, Qin JY, Tian CP, Yan XF, Dong FG, Cheng ZQ, et al. Tubulin inhibitors: pharmacophore modeling, virtual screening and molecular docking. *Acta Pharmacol Sin*. 2014;35(7):967-79. doi: 10.1038/aps.2014.34.
21. JAYARAJ RL, Ranjani V, Manigandan K, Elangovan N. In silico docking studies to identify potent inhibitors of alpha-synuclein aggregation in Parkinson Disease. *Asian Journal of Pharmaceutical and Clinical Research*. 2013:127-31.
22. Rabiei Z, Hojjati M, Rafieian-Kopaeia M, Alibabaei Z. Effect of *Cyperus rotundus* tubers ethanolic extract on learning and memory in animal model of Alzheimer. *Biomedicine & Aging Pathology*. 2013;3(4):185-91. doi: 10.1016/j.biomag.2013.08.006
23. Ayipo YO, Ahmad I, Alananzeh W, Lawal A, Patel H, Mordi MN. Computational modelling of potential Zn-sensitive non- $\beta$ -lactam inhibitors of imipenemase-1 (IMP-1). *J Biomol Struct Dyn*. 2022:1-21. doi: 10.1080/07391102.2022.2153168
24. Zhou X, Smith QR, Liu X. Brain penetrating peptides and peptide-drug conjugates to overcome the blood-brain barrier and target CNS diseases. *Wiley interdisciplinary reviews Nanomedicine and nanobiotechnology*. 2021;13(4):e1695. doi: 10.1002/wnan.1695.
25. Pires DE, Blundell TL, Ascher DB. pkCSM: Predicting Small-Molecule Pharmacokinetic and Toxicity Properties Using Graph-Based Signatures.

- J Med Chem. 2015;58(9):4066-72. doi: 10.1021/acs.jmedchem.5b00104.
26. Drwal MN, Banerjee P, Dunkel M, Wettig MR, Preissner R. ProTox: a web server for the in silico prediction of rodent oral toxicity. *Nucleic Acids Res.* 2014;42(Web Server issue):W53-8. doi: 10.1093/nar/gku401.
  27. Zadorozhnyi PV, Kiselev VV, Kharchenko AV. In silico toxicity evaluation of Salubrinol and its analogues. *European journal of pharmaceutical sciences: official journal of the European Federation for Pharmaceutical Sciences.* 2020;155:105538. doi: 10.1016/j.ejps.2020.105538.
  28. Ahmad I, Jadhav H, Shinde Y, Jagtap V, Girase R, Patel H. Optimizing Bedaquiline for cardiotoxicity by structure based virtual screening, DFT analysis and molecular dynamic simulation studies to identify selective MDR-TB inhibitors. *In silico pharmacology.* 2021;9(1):23. doi: 10.1007/s40203-021-00086-x.
  29. Patel HM, Ahmad I, Pawara R, Shaikh M, Surana S. In silico search of triple mutant T790M/C797S allosteric inhibitors to conquer acquired resistance problem in non-small cell lung cancer (NSCLC): a combined approach of structure-based virtual screening and molecular dynamics simulation. *J Biomol Struct Dyn.* 2021;39(4):1491-505. doi: 10.1080/07391102.2020.1734092.
  30. Patel HM, Shaikh M, Ahmad I, Lokwani D, Surana SJ. BREED based de novo hybridization approach: generating novel T790M/C797S-EGFR tyrosine kinase inhibitors to overcome the problem of mutation and resistance in non small cell lung cancer (NSCLC). *J Biomol Struct Dyn.* 2021;39(8):2838-56. doi: 10.1080/07391102.2020.1754918.
  31. Kalibaeva G, Ferrario M, Ciccotti G. Constant pressure-constant temperature molecular dynamics: A correct constrained NPT ensemble using the molecular virial. *Molecular Physics.* 2003;101(6):765-78. doi: 10.1080/0026897021000044025
  32. Zrieq R, Ahmad I, Snoussi M, Noumi E, Iriti M, Algahtani FD, et al. Tomatidine and Patchouli Alcohol as Inhibitors of SARS-CoV-2 Enzymes (3CLpro, PLpro and NSP15) by Molecular Docking and Molecular Dynamics Simulations. *Int J Mol Sci.* 2021;22(19). doi: 10.3390/ijms221910693.
  33. Gidaro MC, Alcaro S, Secci D, Rivanera D, Mollica A, Agamennone M, et al. Identification of new anti-Candida compounds by ligand-based pharmacophore virtual screening. *J Enzyme Inhib Med Chem.* 2016;31(6):1703-6. doi: 10.3109/14756366.2016.1156103.
  34. Kumar R, Bavi R, Jo MG, Arulalapperumal V, Baek A, Rampogu S, et al. New compounds identified through in silico approaches reduce the alpha-synuclein expression by inhibiting prolyl oligopeptidase in vitro. *Sci Rep.* 2017;7(1):10827. doi: 10.1038/s41598-017-11302-0.
  35. Ouassaf M, Abul Qais F, Belaidi S, Bakhouch M, Mohamed AS, Chtita S. Combined Pharmacophore Modeling, 3D-QSAR, Molecular Docking and Molecular Dynamics Study on Indolyl-aryl-sulfone Derivatives as New HIV1 Inhibitors. *Acta chimica Slovenica.* 2022;69(2):489-506. doi: 10.17344/acsi.2022.7427.
  36. Li T, Guo R, Zong Q, Ling G. Application of molecular docking in elaborating molecular mechanisms and interactions of supramolecular cyclodextrin. *Carbohydrate polymers.* 2022;276:118644. doi: 10.1016/j.carbpol.2021.118644.
  37. Daoud NE, Borah P, Deb PK, Venugopala KN, Hourani W, Alzweiri M, et al. ADMET Profiling in Drug Discovery and Development: Perspectives of In Silico, In Vitro and Integrated Approaches. *Current drug metabolism.* 2021;22(7):503-22. doi: 10.2174/1389200222666210705122913.
  38. Nendza M, Müller M. Screening for low aquatic bioaccumulation. 1. Lipinski's 'Rule of 5' and molecular size. *SAR QSAR Environ Res.* 2010;21(5-6):495-512. doi:10.1080/1062936X.2010.502295
  39. Islam MR, Awal MA, Khames A, Abourehab MAS, Samad A, Hassan WMI, et al. Computational Identification of Druggable Bioactive Compounds from *Catharanthus roseus* and *Avicennia marina* against Colorectal Cancer by Targeting Thymidylate Synthase. *Molecules.* 2022;27(7). doi: 10.3390/molecules27072089.
  40. Ferrari F, Moretti A, Villa RF. Incretin-based drugs as potential therapy for neurodegenerative diseases: current status and perspectives. *Pharmacology & therapeutics.* 2022;239:108277. doi: 10.1016/j.pharmthera.2022.108277.
  41. Saxena D, Sharma A, Siddiqui MH, Kumar R. Blood Brain Barrier Permeability Prediction Using Machine Learning Techniques: An Update. *Current pharmaceutical biotechnology.* 2019;20(14):1163-71. doi: 10.2174/1389201020666190821145346.
  42. Inoue M, Tanaka Y, Matsushita S, Shimozaki Y, Ayame H, Akutsu H. Xenogeneic-Free Human Intestinal Organoids for Assessing Intestinal Nutrient Absorption. *Nutrients.* 2022;14(3). doi: 10.3390/nu14030438.
  43. Highley MS, Landuyt B, Prenen H, Harper PG, De Bruijn EA. The Nitrogen Mustards. *Pharmacological reviews.* 2022;74(3):552-99. doi: 10.1124/pharmrev.120.000121
  44. Varga-Medveczky Z, Kocsis D, Naszlady MB, Fynagy K, Erdő F. Skin-on-a-Chip Technology for Testing Transdermal Drug Delivery-Starting Points and Recent Developments. *Pharmaceutics.* 2021;13(11). doi: 10.3390/pharmaceutics13111852.
  45. Oso BJ, Oyewo EB, Oladiji AT. Influence of ethanolic extracts of dried fruit of *Xylopiya aethiopica* (Dunal) A. Rich on haematological and biochemical parameters in healthy Wistar rats. *Clinical Phytoscience.* 2019;5(1):1-10. doi:

- 10.1186/s40816-019-0104-4
46. Gajjar ND, Dhameliya TM, Shah GB. In search of RdRp and Mpro inhibitors against SARS CoV-2: Molecular docking, molecular dynamic simulations and ADMET analysis. *Journal of molecular structure*. 2021;1239:130488. doi: 10.1016/j.molstruc.2021.130488
47. Prajapati P, Pandey J, Tandon P, Sinha K, Shimpi MR. Molecular Structural, Hydrogen Bonding Interactions, and Chemical Reactivity Studies of Ezetimibe-L-Proline Cocrystal Using Spectroscopic and Quantum Chemical Approach. *Frontiers in chemistry*. 2022;10:848014. doi: 10.3389/fchem.2022.848014
48. Mukherjee R, Somovilla VJ, Chiodo F, Bruijns S, Pieters RJ, Garssen J, et al. Human Milk Oligosaccharide 2'-Fucosyllactose Inhibits Ligand Binding to C-Type Lectin DC-SIGN but Not to Langerin. *Int J Mol Sci*. 2022;23(23). doi: 10.3390/ijms232314745
49. Stafford KA, Anderson BM, Sorenson J, van den Bedem H. AtomNet PoseRanker: Enriching Ligand Pose Quality for Dynamic Proteins in Virtual High-Throughput Screens. *J Chem Inf Model*. 2022;62(5):1178-89. doi:10.1021/acs.jcim.1c01250